J|A|C|S
ARTICLES
Published on Web 03/12/2005

# $CH_5^+$: Chemistry's Chameleon Unmasked

Keiran C. Thompson, Deborah L. Crittenden, and Meredith J. T. Jordan*

*Contribution from the School of Chemistry, University of Sydney, NSW, Australia, 2006*

Received March 29, 2004; E-mail: m.jordan@chem.usyd.edu.au

***Abstract:*** The nuclear vibrational wave function and zero-point vibrational energy of $CH_5^+$ are calculated using quantum diffusion Monte Carlo techniques on an interpolated potential energy surface constructed from CCSD(T)/aug′-cc-pVTZ ab initio data. From this multidimensional wave function, the vibrationally averaged rotational constants and radial distribution functions for atom−atom distances within the molecule are constructed. It is found that the distributions of all 10 H−H distances are bimodal and identical. The radial distribution functions obtained for the five C−H distances are also identical, but unimodal. The three rotational constants were found to be 3.78, 3.80, and 3.83 $cm^{-1}$. These values indicate that the ground state of $CH_5^+$ is significantly more symmetric than its global minimum energy structure. We conclude that the zero-point motion of $CH_5^+$ renders all five protons equivalent in the ground state and precludes the assignment of a unique structure to the molecule.



## Introduction

Since the discovery of the $CH_5^+$ ion in 1952 by Tal'roze and Lyubimova.[1] there has been much speculation about its structure.[2,3] As the smallest protonated alkane, $CH_5^+$ has been viewed as *the* prototypical nonclassical carbocation[4] and its structure is important in our understanding of many reaction mechanisms.[5] Debate has centered on whether this seemingly simple ion is "fluxional", that is, whether the five $CH_5^+$ protons are equivalent and can exchange freely, or whether there is preference in the quantum ground state for a $C_s$ symmetry structure comprising a more "standard" three-center two-electron bond. The recent observation of the high-resolution infrared spectrum[6] of $CH_5^+$ has further fueled interest in this species. Indeed it has been described as chemistry's *Cheshire Cat*.[7]

Initially, in the absence of experimental and theoretical evidence, all five hydrogens around the central carbon atom were considered equivalent.[8] Early theoretical investigations of the electronic structure of $CH_5^+$ [9−13] suggested it might consist of a pyramidal $CH_3^+$ subunit bound to an $H_2$ molecule, in a $C_s$ symmetric arrangement, $C_s$(I) (Figure 1a). Subsequent electronic structure studies[14−18] identified two other low-energy stationary points on the global $CH_5^+$ potential energy surface (PES)—a $C_s$-symmetric structure, $C_s$(II) (Figure 1b), which acts as a transition state for $H_2$ rotation, and a $C_{2v}$-symmetric structure (Figure 1c), which acts as the transition state for $H_2-CH_3$ proton exchange. High-level calculations by Kutzelnigg and coworkers,[18] with a basis set approaching the basis set limit, showed that the relative energies of the $C_s$(II) and $C_{2v}$ structures were 0.4 and 3.2 kJ/mol, respectively, above the global minimum, $C_s$(I).

Results from ab initio electronic structure calculations are often interpreted classically, in the sense that the "structure" of a molecule is defined as the lowest energy geometry on the Born−Oppenheimer PES. In systems where the global minimum lies at the bottom of a deep well, this "structure" generally corresponds quite closely to that obtained by averaging over the nuclear vibrational wave function. For these systems, the traditional notion of molecular structure as small-amplitude vibrations about a well-defined, rigid backbone[19] is both accurate and useful. However, as has been pointed out previously,[2,17,20] this interpretation is not valid for systems such as $CH_5^+$ which have multiple local minima with low barriers to interconversion. These minima correspond to the 120 permutations of the five identical protons in the structure shown in Figure 1a, all of which are expected to be accessible at the zero-point vibrational energy

(1) Tal'roze, V. L.; Lyubinmova, A. K. *Dokl. Akad. Nauk SSSR* **1952**, *86*, 909.
(2) For a review see: Schreiner, P. R. *Angew. Chem., Int. Ed.* **2000**, *39*, 3239.
(3) For a controversial discussion see: (a) Kramer, G. M. *Science* **1999**, *286*, 1051. (b) Oka, T.; White, E. T. *Science* **1999**, *286*, 1051. (c) Marx, D.; Parrinello, M. *Science* **1999**, *286*, 1051.
(4) Olah, G. A.; Klopman, G.; Schlosberg, R. H. *J. Am. Chem. Soc*, **1969**, *91* 3261.
(5) (a) Olah, G. A.; Rasul, G. *Acc. Chem. Res.* **1997**, *30*, 245. (b) Olah, G. A. *Carbocations and Electrophilic Reactions*; Chemie: Weinheim, 1974. (c) Olah, G. A.; Prakash, G. K. S.; Williams, R. E.; Field, L. D.; Wade, K. *Hypercarbon Chemistry*; Wiley: New York, 1987. (d) Olah, G. A.; Prakash, G. K. S.; Sommer, J. *Superacids*; Wiley: New York, 1985.
(6) White, E. T.; Tang, J.; Oka, T. *Science* **1999**, *284*, 135.
(7) Marx, D.; Parrinello, M. *Science* **1999**, *284*, 59.
(8) Sefcik, M. D.; Henis, J. M. S.; Gaspar, P. P. *J. Chem. Phys.* **1974**, *61*, 4321.
(9) Hariharan, P. C.; Latham, W. A.; Pople, J. A. *Chem. Phys. Lett.* **1972**, *14*, 385.
(10) Dyczmons, V.; Kutzelnigg, W. *Theor. Chim. Acta* **1974**, *33*, 239.
(11) Dyczmons, V.; Staemmler, V.; Kutzelnigg, W. *Chem. Phys. Lett.* **1970**, *5*, 361.
(12) Gamba, A.; Morosi, G.; Simonetta, M. *Chem. Phys. Lett.* **1969** *3*, 20.
(13) van der Lugt, W. T. A. M. *Chem. Phys. Lett.* **1969**, *5*, 385.
(14) Komornicki, A.; Dixon, D. A. *J. Chem. Phys.* **1987**, *86*, 5625.
(15) Raghavachari, K.; Whiteside, R. A.; Pople, J. A.; Schleyer, P. v. R. *J. Am. Chem. Soc.* **1981**, *103*, 5649.
(16) Schleyer, P. v. R.; Carnerio, J. W. de M. *J. Comput. Chem.* **1992**, *13*, 997.
(17) Schreiner, P R.; Kim, S.-J.; Schaefer, H. F., III; Schleyer, P. v. R. *J. Chem. Phys.* **1993**, *99*, 3716.
(18) Müller, H.; Kutzelnigg, W.; Noga, J.; Lopper, W. *J. Chem. Phys.* **1997**, *106*, 1863.
(19) Wilson, E. B., Jr.; Decius, J. C.; Cross, P. C. *Molecular Vibrations*; Dover: New York, 1980.
(20) Scuseria, G. E. *Nature* **1993**, *366*, 512.


**10.1021/ja0482280 CCC: $30.25** 

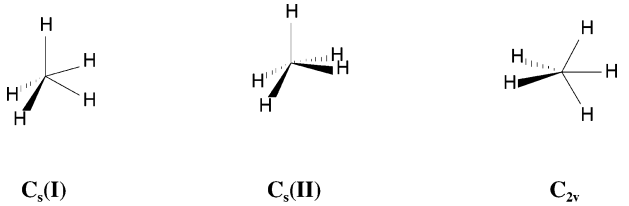


***Figure 1.*** The three low-energy stationary point configurations of $CH_5^+$: (a) the global minimum, $C_s$(I); (b) the transition state for $H_2$ rotation, $C_s$-(II); and (c) the transition state for $H_2-CH_3$ proton exchange, $C_{2v}$.

of the molecular ion. As a result, the nuclear vibrational wave function is unlikely to remain strongly localized to any particular well.

Marx and Parrinello were the first to move beyond a classical view of the structure of $CH_5^+$. They performed both ab initio path integral molecular dynamics calculations,[21] in which the nuclear vibrational and electronic wave functions were calculated simultaneously, and standard Car−Parrinello molecular dynamics calculations,[22] in which the nuclei were treated classically. It was concluded that, although $CH_5^+$ is a fluxional molecule which undergoes hydrogen scrambling and pseudorotations, the quantum ground state is nevertheless dominated by configurations in which an $H_2$ moiety is attached to a $CH_3^+$ group.[21] In a later comment, Marx and Parrinello indicated the possibility that their simulation run may not have been long enough to lead to complete hydrogen scrambling,[3c] an observation which is supported by our results.

Bunker and co-workers[23] have performed quantum vibrational dynamics calculations with a model Hamiltonian based on accurate $CH_5^+$ ab initio data, but restricting the nuclear degrees of freedom to the two lowest frequency modes. In particular, their model did not allow for proton exchange between the $H_2$ and $CH_3^+$ subunits.

In the present work we pin down the chameleon-like nature of $CH_5^+$ by using quantum diffusion Monte Carlo (QDMC)[24−27] to calculate the zero-point energy of the $CH_5^+$ ground state, its exact ground-state nuclear vibrational wave function, and associated rotational constants on a PES interpolated from high-quality ab initio data.

For a six-atom system with large-amplitude motions and many low-lying minima, such as $CH_5^+$, we are aware of only three means of representing the PES: direct ab initio calculation of the potential energy every time it is required, fitting to a functional form or interpolation. Direct ("on-the-fly") calculation of the potential energy in a QDMC simulation is not feasible at high levels of ab initio theory because of the number potential energy evaluations required. Direct dynamics calculations, however, have been carried out on $CH_5^+$ using density functional theory to evaluate the potential energy.[21,28] Fitting the PES to a functional form is also problematic: incorporating the full 5-fold nuclear symmetry is difficult and the actual parametrization of the PES is arbitrary. An analytic PES for $CH_5^+$ has recently been obtained by fitting a multinomial expression to MP2/cc-pVTZ electronic energies and gradients calculated at configurations determined from classical direct dynamics calculations.[29] In this work we use the modified Shepard interpolation scheme of Collins and co-workers,[30−32] as implemented in the Grow 2.2 package,[33] to define the $CH_5^+$ PES, noting that Bettens[34] has recently demonstrated the power of combining this method with accurate ab initio electronic structure calculations and QDMC for the $CH_3F$ molecule.

The next section presents the technical details of the calculations employed here. This is followed by a presentation of the results and a discussion of their interpretation, and finally our conclusions. The ab initio data used to construct the $CH_5^+$ PES may be obtained as Supporting Information.

## Computational Methods

There are three types of calculations involved in this work: the development of the interpolated PES, the ab initio electronic structure calculations, and the QDMC calculations of the nuclear vibrational energy and wave function.

**PES Interpolation.** The modified Shepard interpolation scheme developed by Collins and co-workers[30−32] has been described in detail previously. For details we refer the reader to a recent review.[35] Briefly, the potential energy, $V$, is constructed as a weighted sum of second-order Taylor polynomials about data points in a PES "data set":

$$V(Z) = \sum_i w_i(Z) T_i(Z)$$

The coordinates $Z$ are linear combinations of reciprocal bond lengths, chosen so as to be maximally independent at each data point.[31] Each Taylor polynomial $T_i$ requires the energy, first and second derivatives of the potential, which are obtained from ab initio calculations. The $w_i$ are normalized weight functions that ensure $V(Z)$ has continuous first derivatives and passes exactly through the data points. The sum is taken over all data points and their images under the action of the complete nuclear permutation (CNP) group. This ensures that the interpolated potential energy given by $V(Z)$ is invariant to relabeling of identical atoms, in this case the five hydrogens.

An essential feature of the interpolation scheme of Collins and co-workers is that the PES is "grown" in an iterative fashion: each iteration consists of a dynamics calculation, the selection of new data points, and the calculation of ab initio data at these selected molecular configurations. This cycle is continued until some observable calculated on the interpolated PES ceases to change. In this sense the resulting interpolated PES is adapted to the particular choice of observable, and there is no guarantee that a data set for which one observable has converged will be sufficient for some other observable.

In a recent study, Bettens[34] used the set of walkers from the QDMC calculation at each iteration as a source of new molecular configurations. In this study we have used classical trajectories to generate a sample of new molecular configurations from which "the best" points are chosen. Previous applications of the modified Shepard interpolation scheme to reactive systems have also used classical trajectories to sample molecular configuration space.[35−38] Classical trajectory sampling involved calculating five classical trajectories, using a velocity-Verlet algorithm with a time step of 0.001 au and microcanonical sampling of the initial conditions at total energies of 0.005, 0.01, 0.015, 0.02,

(21) Marx, D.; Parrinello, M. *Nature* **1995**, *375*, 216.
(22) Marx D.; Savin, A. *Angew. Chem., Int. Ed.* **1997**, *36*, 2077.
(23) East, A. L. L.; Kolbuszewski, M.; Bunker, P. R. *J. Phys. Chem. A* **1997**, *101*, 6746.
(24) Anderson, J. B. *J. Chem. Phys.* **1975**, ***63***, 1499
(25) Coker, D. F.; Watts, R. O. *Mol. Phys.* **1986**, ***58***, 1113.
(26) Suhm, M. A.; Watts, R. O. *Phys. Rep.* **1991**, ***204***, 293.
(27) Lewerenz, M. *J. Chem. Phys.* **1996**, ***104***, 1028.
(28) Tse, J. S.; Klug, D. D. *Phys. Rev. Lett.* **1995**, *74*, 876.
(29) Brown, A.; Braams, B. J.; Christoffel, K.; Jin, Z.; Bowman, J. M. *J. Chem. Phys.* **2003**, *119*, 8790. Brown, A.; McCoy, A. B.; Braams, B. J.; Zhong, J.; Bowman, J. M. *J. Chem. Phys.* **2004**, 121, 4105.
(30) Jordan, M. J. T.; Thompson, K. C.; Collins, M. A. *J. Chem. Phys*. **1995**, *102*, 5647.
(31) Thompson, K. C.; Jordan, M. J. T.; Collins, M. A. *J. Chem. Phys.* **1998**, *108*, 8302.
(32) Bettens, R. P. A.; Collins, M. A. *J. Chem. Phys*. **1999**, *111*, 816.
(33) Thompson, K. C.; Crittenden, D. L.; Jordan, M. J. T.; Bettens, R. P. A.; Collins, M. A. Grow 2.2; for further details please contact the authors.
(34) Bettens, R. P. A. *J. Am. Chem. Soc*. **2003**, *125*, 584.
(35) Collins, M. A. *Theor. Chem. Acc*. **2002**, *108*, 313 and references therein.

0.025, 0.03, 0.035, 0.04, and 0.045 $E_h$ above the global minimum energy (Figure 1a). The classical trajectories were propagated for 200 000 time steps (approximately 5ps) and trajectory configurations were saved every 50 time steps and then sampled to provide further data points for the PES data set. The trajectory total energy was incremented by 0.005 $E_h$ after 20 data points were added to the PES data set. Similarly to the calculations of Bettens,[34] the alternating *h-weight*[30] and *rms*[39] scheme was used to select molecular configurations to become new interpolation data points. This strategy was designed to "build up" the $CH_5^+$ PES from low energy to high energy in an attempt to ensure that configuration space in the region of the global minimum was adequately sampled. The interpolation scheme itself introduces small errors in the PES.[30] Despite this, classical trajectories calculated during the growth of the PES conserved energy to better than $2 \times 10^{-7}$ $E_h$.

The five equivalent hydrogens in $CH_5^+$ lead to a 120-fold increase in the size of the data set. In effect, our largest PES has 21 480 data points, which is equivalent to 2.3 data points per degree of freedom. Previous work suggests that the modified Shepard interpolation would be expected to be extremely accurate in such circumstances.[40]

The initial $CH_5^+$ PES was defined by the single global minimum energy configuration, $C_s$(I) (Figure 1a), and its 120 symmetry-equivalent structures.

**Ab Initio Calculations.** Calculations were carried out using the coupled-cluster method with single and double excitations and with noniterative inclusion of triple excitations, CCSD(T).[41−44] The Huzinage−Dunning correlation consistent valence triple-split basis set with diffuse functions on non-hydrogen atoms (aug′-cc-pVTZ),[45−48] as implemented in the Gaussian98 package,[49] was used for all ab initio calculations. Only the valence electrons were explicitly correlated. First and second derivatives of the energy were obtained by numerical differentiation, using central differences. A step size of 0.004 bohr was used, which implies an error in the second derivatives of order 0.02 kJ $mol^{-1}$ $bohr^{-2}$.

Our choice of basis was motivated by the compromise between accuracy and computational cost. The aug′-cc-pVTZ basis set is 5s4p2d2f on carbon and 3s2p1d on hydrogen. Despite Schreiner and co-workers' findings that d-functions on the hydrogen atoms made essentially no difference to the energy,[17] we were concerned about accuracy at geometries far from the global minimum. Nevertheless, our basis is somewhat short of the basis set limit calculations of Müller et al.[18] From their work, it follows that our choice of electron correlation method and basis set imply absolute errors in the energy of up to 25 m$E_h$, or ∼65 kJ/mol. However, relative errors in the energies of the $C_s$(II) and $C_{2v}$ structures (Figure 1b,c) are expected to be less than 0.4 kJ/mol.[18]

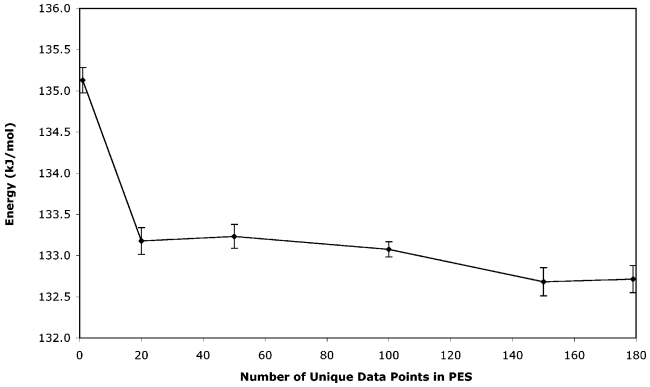


***Figure 2.*** $CH_5^+$ ground-state zero-point energy (kJ/mol) calculated from PES interpolated from 1, 20, 50, 100, 150, and 179 unique data points. Error bars represent two standard errors of the mean, as calculated from 20 independent QDMC simulation tuns.

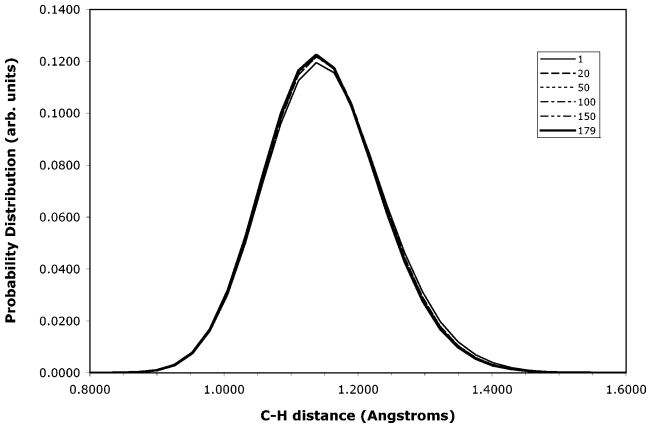


***Figure 3.*** Averaged C−H radial distribution functions for the $CH_5^+$ ground-state wave function calculated from PES interpolated from 1, 20, 50, 100, 150, and 179 unique data points.

**Quantum Diffusion Monte Carlo Calculations.** The ground-state zero-point energy, the nuclear vibrational wave function, and the $CH_5^+$ rotational constants were determined using the discrete weight quantum diffusion Monte Carlo algorithm[24−27] with energies calculated from an interpolated PES. All QDMC calculations involved 1000 replicas starting from an initial ensemble generated by random displacements of up to 0.5 bohr in the Cartesian coordinates of the global minimum energy configuration, $C_s$(I) (Figure 1a). The ensemble was allowed to equilibrate for 10 000 steps and statistics were then collected for a further 20 000 time steps. A step size of 1 au was used throughout.

Convergence of the PES was monitored, in terms of ground-state zero-point energy, ground-state nuclear vibrational wave function, and ground-state rotational constants, after 1, 20, 50, 100, 150, and 179 unique data points had been added to the PES by performing 20 independent QDMC simulation runs. The ground state, or zero-point, energy on each PES was calculated as the average of the 20 values obtained. The uncertainties quoted in the next section are twice the standard error of the mean, that is, $2\sigma/\sqrt{N}$, where $\sigma$ is the standard deviation of the 20 energy values, and $N = 20$.

Wave function histograms were obtained by binning the atom−atom distances in each replica at every time step of the simulation run and averaging over the 20 simulation runs. These one-dimensional histograms correspond to $4\pi r^2\psi(r)$, where $r$ is the particular bond length in question and $\psi$ is the molecular wave function.[25] The bond length distributions presented below were obtained by scaling by $1/4\pi r^2$ and then squaring to yield $|\psi(r)|^2$. Figures 3 and 4 should be interpreted to mean that the height of the curve represents the probability of the

(36) Brouard, M.; Burak, I.; Minayev, D.; O'Keeffe, P.; Vallance, C.; Aoiz, F. J.; Bañares, L.; Castillo, J. F.; Zhang, D. H.; Collins M. A. *J. Chem. Phys.* **2003**, *118*, 1162.
(37) Moyano, G. E.; Collins, M. A. *J. Chem. Phys.* **2003**, *119*, 5510.
(38) Collins, M. A.; Radom, L. *J. Chem. Phys.* **2003**, *118*, 6222.
(39) Thompson, K. C.; Collins, M. A. *J. Chem. Soc., Faraday Trans.* **1997**, *93*, 871.
(40) Bettens, R. P. A.; Collins, M. A. *J. Chem. Phys.* **1998**, *109*, 9728.
(41) Purvis, G. D., III; Bartlett, R. J. *J. Chem. Phys.* **1982**, *76*, 1910.
(42) Urban, M.; Noga, J.; Cole, S. J.; Bartlett, R. J. *J. Chem. Phys.* **1985**, *83*, 4041.
(43) Bartlett, R. J.; Watts, R. J.; Kucharski, S. A.; Noga, J. *Chem. Phys. Lett.* **1990**, *165*, 513.
(44) Raghavachari, K.; Trucks, G. W.; Pople, J. A.; Head-Gordon, M. *Chem. Phys. Lett.* **1989**, *157*, 479.
(45) Dunning, T. H., Jr. *J. Chem. Phys*, **1989**, *90*, 1007.
(46) Kendall, R. A.; Dunning, T. H., Jr. *J. Chem. Phys.* **1993**, *96*, 1358.
(47) Woon, D. E.; Dunning, T. H., Jr. *J. Chem. Phys.* **1993**, *98*, 1358.
(48) Davidson, E. R. *Chem. Phys. Lett.* **1996**, *260*, 514.
(49) Frisch, M. J.; Trucks, G. W.; Schlegel, H. B.; Scuseria, G. E.; Robb, M. A.; Cheeseman, J. R.; Zakrzewski, V. G.; Montgomery, J. A., Jr.; Stratmann, R. E.; Burant, J. C.; Dapprich, S.; Millam, J. M.; Daniels, A. D.; Kudin, K. N.; Strain, M. C.; Farkas, O.; Tomasi, J.; Barone, V.; Cossi, M.; Cammi, R.; Mennucci, B.; Pomelli, C.; Adamo, C.; Clifford, S.; Ochterski, J.; Petersson, G. A.; Ayala, P. Y.; Cui, J.; Morokuma, K.; Malick, D. K.; Rabuck, A. D.; Raghavachari, K.; Foresman, J. B.; Cioslowski, J.; Ortiz, J. V.; Baboul, A. G.; Stefanov, B. B.; Liu, G.; Liashenko, A.; Piskorz, P.; Komaromi, I.; Gomperts, R.; Martin, R. L.; Fox, D. J.; Keith, T.; Al-Laham, M. A.; Peng, C. Y.; Nanayakkara, A.; Gonzalez, C.; Challacombe, M.; Gill, P. M. W.; Johnson, B.; Chen, W.; Wong, M. W.; Andres, J. L.; Gonzalez, C.; Head-Gordon, M.; Replogle, E. S.; Pople, J. A. *Gaussian 98*; Gaussian, Inc.: Pittsburgh, PA, 1998.

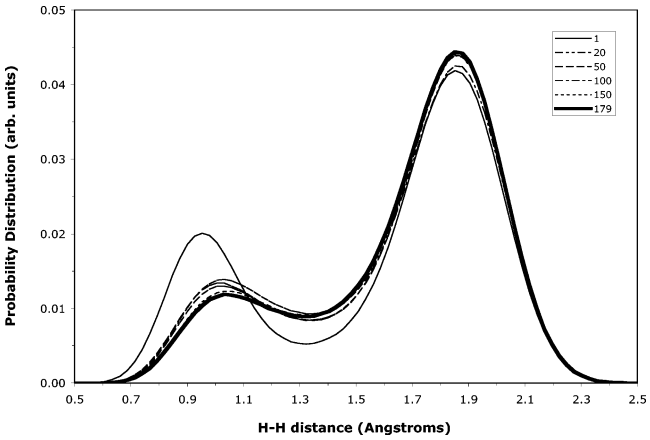


***Figure 4.*** Averaged H−H radial distribution functions for the $CH_5^+$ ground-state wave function calculated from PES interpolated from 1, 20, 50, 100, 150, and 179 unique data points.

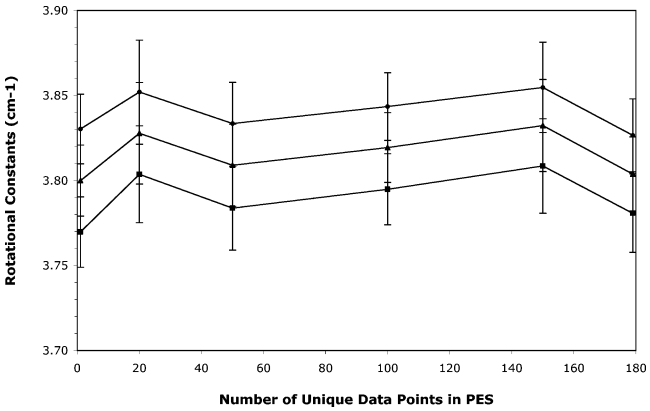


***Figure 5.*** $CH_5^+$ ground-state rotational constants (GHz) calculated from PES interpolated from 1, 20, 50, 100, 150, and 179 unique data points. Error bars represent two standard errors of the mean, as calculated from 20 independent QDMC simulation runs.

molecule being in a configuration with the corresponding value for that bond length.

Vibrationally averaged rotational constants were obtained by rotating the Cartesian coordinates of each replica into the Eckart frame[51] of the $C_s$(I) minimum energy structure of Figure 1a, and accumulating the resulting inverted moment of inertia tensor using the descendant weighting algorithm.[25,26] Descendents were followed for 110 000 steps, with a new generation spawned every 400 steps, so that 20 generations were followed simultaneously during the 20 000 step convergence calculations. All 120 permutations of each replica were included in the resulting average of inverted moment of inertia tensors. Again, the uncertainties quoted below represent twice the standard error of the mean, as calculated from the 20 independent QDMC simulation runs.

All calculations reported here were carried out using facilities at the Australian Partnership for Advanced Computing (APAC).

## Results and Discussion

The zero-point energy of $CH_5^+$ as a function of the number of distinct data points that define the global PES is illustrated in Figure 2. From this figure, we observe that the PES has converged with respect to the calculation of the ground-state energy to within ± 0.5 kJ/mol by 150 data points. The converged fully anharmonic zero-point energy on our interpolated PES was 132.72 ± 0.16 kJ/mol, significantly lower than the CCSD(T)/aug′-cc-pVTZ harmonic zero-point energy of the global minimum energy structure, $C_s$(I) (Figure 1a), which was found to be 134.75 kJ/mol. These results compare with those of Bowman and co-workers:[29] their $CH_5^+$ MP2/cc-pVTZ harmonic zero-point energy at the $C_s$(I) structure was 136.7 kJ/mol and they reported preliminary QDMC calculations suggesting an anharmonic zero-point energy of approximately 131 kJ/mol. The best estimates of the harmonic zero-point energy of the three species illustrated in Figure 1 are 136.8 kJ/mol for $C_s$(I), 136.4 kJ/mol for $C_s$(II), and 132.0 kJ/mol for the $C_{2v}$ structure.[17] Indeed Schreiner et al. scaled their harmonic frequencies by 0.95 in an attempt to estimate anharmonic effects.[17] Here we find that the ratio of the exact anharmonic zero-point energy on the CCSD(T)/aug′-cc-pVTZ interpolated PES to the harmonic zero-point energy is 0.985.

The zero-point energy appears to converge quickly, both in terms of number of QDMC diffusion steps and the size of the data set defining the PES. A more sensitive measure of PES convergence is provided by the nuclear vibrational wave function itself.

As a means of comprehending the 12-dimensional $CH_5^+$ wave function, $\psi$, we construct the distributions of distances between pairs of atoms. These one-dimensional slices through $|\psi(r)|^2$, or radial distribution functions, for the C−H and H−H distances are shown in Figures 3 and 4, respectively. The C−H radial distribution function is observed to converge by 50 data points, and the H−H radial distribution function converges by approximately 150 unique data points.

During the initial stages of the QDMC simulation, the labeled H−H and C−H radial distribution functions were distinguishable. Each H−H and C−H distribution function was unimodal, with a peak in the relative probability corresponding to the classical H−H or C−H distance in the $C_s$(I) configuration. The combined H−H radial distribution function was, therefore, multimodal, with a peak at each H−H distance that corresponded to a classical H−H bond length. Similarly, the combined C−H radial distribution function initially reflected the classical C−H bond lengths. As the QDMC simulation progressed, the labeled H−H and C−H radial distribution functions converged and became indistinguishable, indicating that complete scrambling of the hydrogen atoms had occurred. The final, averaged C−H and H−H radial distribution functions are illustrated in Figures 3 and 4, respectively, for the different PES considered.

The C−H radial distribution functions illustrated in Figure 3 are unimodal. This implies that the five protons are, on average, equidistant from the central carbon atom.

Figure 4 indicates that the H−H distribution function is bimodal. The bimodal distribution is consistent with the $C_s$(I) and $C_s$(II) structures illustrated in Figure 1, with the peak at short H−H distance, approximately 0.95 Å, representing the $H_2$ moiety, and the peak at 1.8 Å representing nonbonded interactions. It is instructive to observe the change in H−H distributions as the size of the potential energy data set is increased. While the "one-point" interpolated PES gives a distribution with a clear $CH_3{\cdot}H_2$ structure, the distributions from more complete PES are significantly lower in the 0.95 Å region and correspondingly higher in the intermediate 1.1−1.5 Å region. The ratio of the two peaks in the final H−H distribution is 1:3.6 and the saddle at 1.3 Å is only 25% lower than the first peak. These features imply that the protons are not confined to the $C_s$(I) local minima and that there is significant density at configurations far from "equilibrium".

(50) Illustrations generated with VMD: Humphrey, W.; Dalke, A.; Schulten, K. VMD−Visual Molecular Dynamics. *J. Mol. Graphics* **1996**, *14.1*, 33−38.

(51) Pickett, H. M.; Strauss, H. L. *J. Am. Chem. Soc.* **1970**, *92*, 7281.

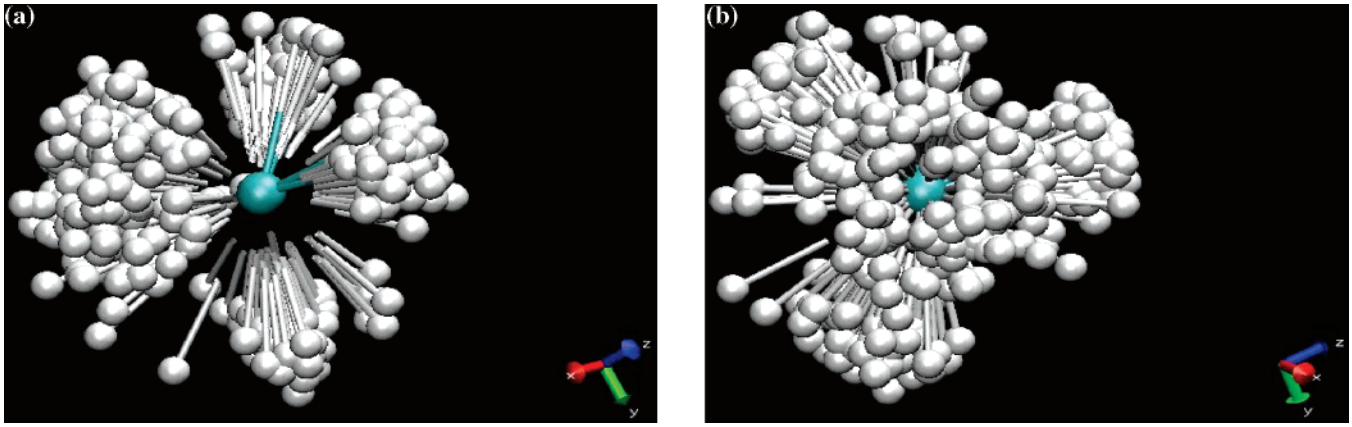


***Figure 6.*** Two views of a superposition of 83 high-probability walkers from a QDMC run on the 179-point PES.

The results obtained here are consistent with the earlier calculations of Marx and Parrinello.[21] They found that the H−H radial distribution function at 5 K was multimodal and the C−H radial distribution function could be deconvolved to a bimodal distribution.

The convergence of the three $CH_5^+$ rotational constants, *A*, *B*, and *C*, are illustrated in Figure 5 as a function of the number of unique data points in the PES data set. These values appear to converge for a PES defined by approximately 20 unique data points. The converged values for the $CH_5^+$ ground state are $A = 3.83 \pm 0.02$ cm$^{-1}$, $B = 3.80 \pm 0.02$ cm$^{-1}$, and $C = 3.78 \pm 0.02$ cm$^{-1}$. The corresponding values for the $C_s$(I) minimum energy structure are 4.30, 3.93, and 3.62 cm$^{-1}$. The similarity of the three rotational constants suggests that the ground-state $CH_5^+$ structure is very nearly a symmetric top and significantly more symmetric than the minimum energy $C_s$(I) structure, Figure 1a. These results further support the notion that there is complete hydrogen scrambling in the $CH_5^+$ ground state, i.e., that all five protons are statistically equivalent.

Figure 6 shows two views of the superposition[50] of the 83 highest probability configurations from an ensemble of 1000 walkers equilibrated on the final, 179-point PES. Each geometry was rotated into the Eckart frame[51] of the $C_s$(I) structure of Figure 1a. In Figure 6a, the three "methyl" protons are clearly distinguishable to the right of the central carbon, and the $H_2$ subunit is a larger swarm of atoms on the left. Panel b, as indicated by the axes in the lower right-hand corner of both panels, is a 90° rotation of panel a, in which the methyl structure is still clearly visible. Also visible in panel b, however, is the structure of the $H_2$ subunit: there appears to be some bias toward the $C_s$(I) structure but the ring of atoms in the foreground, with the central carbon visible through the hole in the center, indicates that $H_2$ rotation is essentially unhindered in the ground state.

The atoms directly above the carbon in panel a can be seen in panel b to lie between the methyl positions. As the number of walkers included in the superposition was increased, these lower probability configurations filled out the remaining empty spaces and the carbon atom was obscured. The resulting image was largely featureless and is not included. Nevertheless, these far from equilibrium configurations represent snapshots of the proton scrambling mechanism in $CH_5^+$.

With the observation of $H_2$ rotation, the implications of Fermi−Dirac statistics should be considered. The present calculations are performed within the Born−Oppenheimer approximation and ignore nuclear spin statistics.

## Conclusion

The classical notion of molecular structure does not apply to $CH_5^+$. Rather than remaining localized in a single energy minimum on the PES, $CH_5^+$ can only be described by a nuclear vibrational wave function that accesses large areas of conformational space. All five hydrogen atoms in $CH_5^+$ possess identical C−H and H−H radial distribution functions within the nuclear vibrational wave function and are quantum mechanically equivalent. There is substantial proton scrambling, even at 0 K.

The ground-state $CH_5^+$ wave function does have some $C_s$(I) character, as evidenced by the bimodal character of the H−H radial distribution function; however, there is considerable delocalization of the protons and the calculated rotational constants suggest that the $CH_5^+$ ground-state structure is more symmetric than the $C_s$(I) global minimum energy configuration. The $CH_5^+$ chameleon has been unmasked, and it is indeed a fluxional molecule.

**Acknowledgment.** D.L.C. acknowledges the financial support of an Australian Postgraduate Research Award. This work has also been supported by Large Grant A00104447 from the Australian Research Council and by grants of computer time from the Australian Partnership in Advanced Computing (APAC) National Merit Allocation Scheme.

**Note Added in Proof:** Since submission of this manuscript a full-dimensional MP2/cc-pVTZ PES has been constructed by McCoy and coworkers by fitting 20633 ab initio data points to a polynomial expansion in the symmetry coordinates for $CH_5^+$ using 2303 coefficients [McCoy, A. B.; Braams, B. A.; Brown, A.; Huang, X.; Jin, Z.; Bowman, J. M *J. Phys. Chem. A* **2004**, *108*, 4991]. This surface has an rms fitting error of 51.0 cm$^{-1}$. QDMC calculations performed on this PES [Brown, A.; McCoy, A. B.; Braams, B. A.; Jin, Z.; Bowman, J. M. *J. Chem. Phys.* **2004**, *121*, 4105] yield bond-length distributions qualitatively similar to those reported here, with a lower ZPE and a higher average rotational constant.

**Supporting Information Available:** Geometric configurations, energies, gradients, and Hessians of the data points used to construct the $CH_5^+$ PES, as well as the "standard orientation" used for $CH_5^+$. This material is available free of charge via the Internet at http://pubs.acs.org. The Grow 2.2 package, including PES interpolation code, is available from the authors.

JA0482280